Research article

Scenario analysis of PM$_{2.5}$ and ozone impacts on health, crops and climate with TM5-FASST: A case study in the Western Balkans

Claudio A. Belis [a],[*], Rita Van Dingenen [a], Zbigniew Klimont [b], Frank Dentener [a]

[a] *European Commission, Joint Research Centre, Via Fermi 2749, 21027, Ispra, VA, Italy*
[b] *International Institute for Applied System Analysis (IIASA), Laxenburg, Austria*

ARTICLE INFO

ABSTRACT

The Western Balkans (WB) is a region in South-East Europe where the alignment of national legislations and policies with those of the European Union (EU) is in progress with the prospect of achieving the EU membership. Such process is crucial for air quality management considering that the levels of air pollution in this area are among the highest of Europe and affect neighbouring regions. With the aim of informing the design of air quality policies in the WB, the TM5-FAst Scenario Screening Tool (TM5- FASST) was used to estimate the trends of air quality (PM 2.5 and ozone) impacts on health, crops yields and climate from 2000 to 2050. To that end, five ECLIPSE V6b emission scenarios with different assumptions on population growth, deployment of technologies and policies were compared. The measures in the current legislation baseline (CLE) are effective in abating the projected impact of energy, transport and domestic sectors on air quality while they show little effect on agriculture and waste sectors. The implementation of the maximum feasible reduction (MFR) scenarios in the WB would lead to a decrease in the mortality associated with PM 2.5 of 49%–65% in 2050 compared to CLE. On the contrary, no further control (NFC) scenarios would cause an increase in PM 2.5 mortality of 16%–21% in 2050 compared to CLE. The analysis of the mortality associated with transboundary pollution suggests that lack of action would lead to a considerable increase in the impact of WB emissions on neighbouring countries. The MFR scenario would also lead to a reduction of the agricultural losses due to ozone pollution of 38%–90% in 2050 compared to the CLE. The global warming potential on a 20-years' timescale was assessed to estimate the medium term impact of air pollutants' emission reduction on climate. In the CLE it would increase by 110 CO 2 eq Tg by 2050 compared to 2000 and it could be mitigated by measures in line with the Paris Agreement 2°C target and the UN sustainable development goals (e.g. on energy transition and depollution). The scenarios analysed depict a spectre ranging from the maximum benefits of combining ambitious air quality and climate policies to the impact of no implementing the currently adopted ones that provides a reference framework for the development of sustainable policies in the region.

1. Introduction

Exposure to air pollution is the main environmental risk of early death and in 2019 is estimated to have contributed to 5.9–7.5 million premature deaths globally, two thirds of which are attributable to PM$_{2.5}$ and ozone (O$_3$) (Health Effects Institute HEI, 2020). During the last decades premature deaths attributable to outdoor PM$_{2.5}$ exposure in low- and middle-income countries in East Asia, South Asia, Africa, and the Middle East are growing, while PM$_{2.5}$ concentrations in high-income countries, most of which are in Europe and North America, have steadily decreased in the same period (Burnett and Cohen, 2020).

Exposure to high levels of ambient air pollutants can also cause damage to agricultural crops which range from foliar injury, reduced growth and yield, to premature death of the plant (Grulke and Heath, 2020). Due to its oxidative action, O$_3$ is the main pollutant affecting plants throughout the growing season and particularly between June and August, when the levels of this pollutant reach their maxima (Emberson, 2020). Wheat, soybean and cotton are the most sensitive crops to O$_3$ damage and global-scale assessments estimated between 4% and 15% relative yield reductions for wheat, maize, soybean and rice in

2000 (Hollaway et al., 2012; Avnery et al., 2011). Projected relative yield reductions for maize and rice between 2005 and 2050 are within that range, with values reaching 10% in Middle East, India and China while maximum values in Europe and US are about 4% (Chuwah et al., 2015).

Air pollutants also interact with the atmosphere's radiative balance, either by cooling or warming (Monks et al., 2015). Particulate matter in general consist of a mixture of scattering components (e.g. ammonium-sulfate or –nitrate) and absorbing species (e.g. black carbon, iron-rich suspended dust) and their relative abundances determine the net radiative forcing. Globally, the best estimate of total anthropogenic aerosol effective radiative forcing (including aerosol-radiation and excluding aerosol-cloud interactions and the impact of black carbon on snow and ice albedo) is -0.3 (-0.6 to 0.0) W/m^2 over the period 1750–2014 (IPCC, 2021). O_3 also has a considerable global mean radiative forcing estimated at $+0.47$ (0.24–0.71) W/m^2 (stratospheric and tropospheric) between 1750 and 2019, dominated by tropospheric ozone changes (IPCC, 2021). Between 1850 and 2000, the anthropogenic precursors of O_3, methane (CH_4), nitrogen oxides (NOx), carbon monoxide (CO) and non-methane volatile organic compounds (NMVOC) were responsible for $44 \pm 12\%$, $31 \pm 9\%$, $15 \pm 3\%$ and $9 \pm 2\%$ respectively, of the O_3 radiative forcing (Stevenson et al., 2013). In addition, these compounds affect the abundance of the OH radical and consequently the lifetime of CH_4. Therefore, impacts on climate of O_3 precursors go beyond the changes in O_3 levels and often occur over different timescales (Monks et al., 2015). Climate-smart air quality policies, focusing on emission sources of net-warming pollutants, may contribute to keeping the global and regional temperature trends within safe limits (Shindell et al., 2012).

The Western Balkans (WB) region covers an area of about 218,750 km^2 and has a population of 19.9 million with a total gross domestic product (GDP) of US\$ (current) 112 billion in 2020 (World Bank, 2021). The WB comprise: Albania, Bosnia and Herzegovina, Kosovo*1, Montenegro, North Macedonia and Serbia and is surrounded by several EU countries, namely Hungary (HU), Bulgaria (BG), Romania (RO), Greece (GR), and Croatia (HR).

The WB region is one of the air pollution hotspots of Europe. Particulate matter (PM$_{10}$ and PM$_{2.5}$), sulfur dioxide (SO$_2$), O$_3$ and nitrogen dioxide (NO$_2$) are the pollutants whose levels are most frequently above the legislation limits (Banja et al., 2020). In particular, the three-year PM$_{2.5}$ average (2016–2018) is above the exposure concentration obligation (20 µg/m^3) in most of the region and the main contributors of this pollutant are coal fuelled power plants and biomass burning for domestic heating (Belis et al., 2019).

The premature deaths directly attributable to air pollution in the WB in 2019 were nearly 30,000, 93% of which associated with PM$_{2.5}$, and its relative mortality per 100,000 inhabitants of nearly 160 more than doubled the EU27 average (EEA, 2021). Air pollution in the WB contributes between 4% and 19% of total premature mortality in 18 selected WB cities and reduces life expectancy by between 0.4 and 1.3 years (UNEP, 2019).

In recent years, the EU has increasingly focused the attention on the WB accession process (European Commission, 2018; European Commission, 2020a) triggering a phase of profound social and legal transformations in the area aimed to align the legislation of these countries with the EU cumulative body of laws (*EU acquis*). Moreover, the launch of the EU Green Deal (EU-GD; European Commission, 2019) has put environmental and climatic issues in the spotlight foreboding further progress of the current *EU acquis* in the coming years. Due to the transboundary nature of environmental pollution, an upstream involvement of the Western Balkans would be highly beneficial for achieving the EU-GD zero pollution ambition in the neighbouring EU member states. For that reason, the European Commission has recently adopted a Green Agenda for the Western Balkans where the main orientations for a sustainable development of the region in line with the EU-GD are depicted (European Commission, 2020b). The Green Agenda

for the Western Balkans focus on the promotion of multimodal transport and modal shift, the use of cleaner fuels and the renovation of the fleet, while the clean energy measures include the transition from coal by promotion of renewables and cleaner fuels and the improvement of the energy efficiency of buildings.

The aim of the study is to analyse the differences in the air quality impacts associated with a variety of policy-relevant scenarios. To that end, we applied an air quality modelling tool to estimate the recent-past and future trends of the air quality impacts on health, crops yields and climate on the basis of socio-economic scenarios describing possible future population growth, the deployment of technologies and the implementation of abatement measures. Special emphasis was placed on the differences between ambitious abatement strategies with respect to the baseline as markers of the maximum achievable benefits, on the one hand, and the consequences of not implementing the adopted measures, on the other hand.

2. Material and methods

2.1. TM5-FASST

The TM5-FAst Scenario Screening Tool (TM5-FASST) is a reduced-form air quality source–receptor model designed to compute global air pollutant-related impacts on human health, agricultural crop production, and short-lived pollutant climate metrics, taking as input annual pollutant emission data aggregated at the national or regional level (Van Dingenen et al., 2018). The TM5-FASST tool is based on linearised emission concentration sensitivities (source-receptor coefficients, SR) originally derived with the full chemistry transport model TM5 (Krol et al., 2005).

Pollutants considered are atmospheric trace gases (O$_3$, SO$_2$, NOx, NMVOCs, NH$_3$ and CH$_4$), and particulate matter. The latter includes primary PM$_{2.5}$ and its components black carbon (BC), organic carbon (OC), sea salt (SS), mineral dust (DU), and secondary components (sulfate, nitrate, and ammonium). For TM5-FASST, 56 emission source regions are defined (Van Dingenen et al., 2018) while the concentrations and impacts are computed on a $1° \times 1°$ gridded domain which is further interpolated to $0.125° \times 0.125°$ resolution to estimate population exposure. In the current version of TM5-FASST, the Western Balkans, including Croatia, are aggregated into a single source region, hence we use common assumptions for the emission scenarios of the individual countries in the WB.

Health impacts are computed for metrics consistent with underlying epidemiological studies (Jerrett et al., 2009; Krewski et al., 2009; Pope III et al., 2002), i.e. population weighted annual mean PM$_{2.5}$ at 35% relative humidity and the seasonal daily maximum 8 h average O$_3$ concentration metric (SDMA8h). Health impacts from PM$_{2.5}$ are calculated, using the integrated exposure-response model (IER) adopted in the Global Burden of Disease (GBD 2017) assessment (Stanaway et al., 2018), as the number of annual premature mortalities from six causes of death: chronic obstructive pulmonary disease (COPD), lung cancer (LC), lower respiratory airway infections (LRI), diabetes mellitus (DM), ischemic heart disease (IHD), and stroke.

Cause-specific excess mortalities are calculated at grid cell level using a population-attributable fraction approach (Murray et al., 2003):

$$\triangle Mort = m_0 . AF . POP \tag{1}$$

$$AF = \frac{(RR - 1)}{RR} \tag{2}$$

where m_0 is the cause-specific all-risk mortality rate (deaths per capita) for the exposed population POP, AF is the fraction of total mortalities attributable to air pollution, and RR is the relative risk of death attributable to a change in population-weighted mean pollutant concentration. For PM$_{2.5}$ exposure, RR is calculated from the IER functions

developed by Burnett et al. (2014):

$$RR_{PM2.5} = 1 + \alpha\{1 - \exp[-\gamma(PM2.5 - zcf)^\delta]\} \text{ for } PM2.5 > zcf \quad (3)$$

$$RR_{PM2.5} = 1 \text{ for } PM2.5 \leq zcf$$

where α, γ and δ are parameters provided in the abovementioned references and zcf is the counterfactual concentration, i.e. a theoretical minimum exposure level below which there is no excess risk. α, γ, δ, and zcf were obtained from fittings to the median and 95 percentile exposure response curves of 1000 sampled RR's in the range 1–600 $\mu g/m^3$. The fitted parameter values are given in Table S1 of the supplementary material. Our fittings reproduce the IER functions applied in the GBD 2017 assessment (Stanaway et al., 2018) which is an update of the function coefficients used in Van Dingenen et al. (2018).

Mortality due to O_3 exposure is related to COPD, based on a log-linear exposure-response function, using exposure metric and relative risk from GBD 2017. As a sensitivity analysis we also apply the higher metric and relative risk proposed by Turner et al. (2016), as it may have important consequences for transboundary impacts of emission reductions. In the former, the O_3 exposure indicator is the seasonal 8 h mean (SDMA8h) with a RR of 1.06/10 ppb for COPD and a zero-risk threshold (zcf) of 29.1 ppb while in the latter the exposure indicator is the annual 8 h mean (ADMA8h) with a RR equal to 1.14/10 ppb for COPD and a threshold of 26.7 ppb. The approach by Turner et al. provides higher estimates than the GBD2017 because of the higher mortality relative risk and the lower thresholds.

In TM5-FASST the relative yield loss (RYL) of four crops (wheat, maize, rice and soybean) is computed from crop-specific exposure-response functions, expressing it as a function of growing-season-averaged exposure metric. Gridded O_3 crop exposure metrics are overlaid with crop suitability maps for the relevant emission regions in order to obtain regional-mean exposure indices (Van Dingenen et al., 2009, 2018). The O_3 exposure metrics are the three month accumulated concentrations above 40 ppb (AOT40) and seasonal three-month averages of 7 h (M7) and 12 h (M12) daytime concentrations. In this study we denote the latter metrics by Mi which refers to M7 for wheat and rice, and to M12 for maize and soybean. The growing season is defined as the three months centred around mid-growing season. The crop suitability maps defining the crops' spatial distribution and crop-specific growing season are taken from Global Agro-Ecological Zones (GAEZ) methodology and related global dataset (Food and Agriculture Organisation of the United Nations, 2012). Exposure-response functions for AOT40 and Mi are from Mills et al. (2007) and from Wang and Mauzerall (2004) respectively.

TM5-FASST includes a set of pre-computed regional-to-global radiative forcing source-receptor coefficients (RFSR) for a precursor (j) emitted from a region (k) expressing the change in global radiative forcing per unit of pollutant emission. For each emitted pollutant (primary and secondary), the resulting normalised global forcing responses have been used to calculate the region-specific global warming potential (GWP) for a series of time horizons (e.g. 20, 50, 100, 500 years) following Fuglestvedt et al. (2010). A detailed description and validation of the TM5-FASST model and methodology is given by Van Dingenen et al. (2018).

The 2015 annual mean concentrations of $PM_{2.5}$ and O_3 computed with TM5-FASST in the WB are consistent with the CAMS ensemble model estimations for the same year and region (the CAMS model results are used as proxy for data driven validation because they undergo an operational validation procedure). The mean annual average bias (MB) for $PM_{2.5}$ is -0.13 $\mu g/m^3$, the normalised mean bias (NMB) -0.009 and the root mean square error (RMSE) 3.11 $\mu g/m^3$. For O_3, the MB is 3.9 ppb, the NMB 0.10 and the RMSE 4.6 ppb. More details are given in Figures S1 and S2 of the supplementary material. In addition, the TM5-FASST 2015 annual averages of pollutants were compared with measurements from WB sites reported to EIONET and the results are

Table 1

Description of ECLIPSE version 6 b global scenarios used in this study (IIASA, 2021; Klimont et al., in preparation; IEA, 2018).

Scenario	abbreviation	Air quality policy	Climate policy
Current legislation (baseline)	CLE	Current baseline projections according to the IEA World Energy Outlook 2018 New Policy Scenario (NPS[a]) which includes EU 2030 renewable energy and energy efficiency targets and announced energy policies by China, USA, Japan and Korea.	Incorporates only commitments made in the national determined contributions (NDC) under the Paris Agreement.
Maximum technical reduction baseline	MFR base	Stringent policy assuming introduction of best currently available technology and no cost limitations. However, no further technological improvements are foreseen. Same activity drivers as CLE following NPS.	Incorporates only commitments made in the NDCs under the Paris Agreement.
Maximum technical reduction sustainable development (most ambitious scenario)	MFR SDS	Similar to MFR base. However, relies on the most ambitious IEA sustainable development scenario (SDS). Includes outcomes of energy-related SDGs: reducing dramatically premature deaths due to energy-related air pollution and universal access to modern energy by 2030.	Aligned with Sustainable Development Goal #13 and Paris Agreement goal of keeping global average temperature increase below 2 °C.
No further control baseline	NFC base	No new measures beyond 2015–2018. Turnover of stock is included. However, the impact of recent stringent legislation like diesel-gate related measures, low-sulfur fuel for marine vessels and eco-design (e. g. residential heating devices) is not considered. Same activity drivers (NPS) as CLE.	Incorporates only commitments made in the NDCs under the Paris Agreement.
No further control current energy policies (most pessimistic scenario)	NFC CPS	Similar to NFC base. However, relies on IEA current policy scenario (CPS[b]) based on laws and regulations existing as of mid-2018. Excludes the announced policies.	Paris Agreement NDCs are missing implying higher share of fossil fuels and less fuel efficiency than NFC base.

[a] In NPS, fossil fuel subsidies phased out in all net-importing countries, and in net-exporting countries where specific policies have been announced.

[b] In CPS fossil fuel subsidies phased out only in countries that already have relevant policies in place.

discussed in the supplementary material (Figures S3 and S4).

We evaluate pollutant emissions and their impacts aggregated over all source sectors (described in section 2.2), as well as the share of individual sectors by subtracting sector emissions one by one from the total, and computing the difference in outcome with the total-emissions outcome (more details in Van Dingenen et al., 2018; Belis et al., 2020).

2.2. Emission scenarios

With the aim to evaluate past and future impact projections under different air quality and related climate policies, we used the global ECLIPSE emission scenarios, developed using the GAINS model (Amann et al., 2011; Klimont et al., 2017), from 2000 to 2050. The ECLIPSE V6b adopted in this study (Table 1) is the most recent emission dataset of this series (IIASA, 2021; Klimont et al., in preparation). The ECLIPSE V6b scenarios consider anthropogenic emissions of SO_2, NOx, $PM_{2.5}$ (BC, particulate organic matter, other primary $PM_{2.5}$), NMVOC, CO, NH_3 and CH_4 with 0.5×0.5 deg. spatial resolution and annual and monthly temporal detail. The annual emissions are split by sectors: energy production (ENE), industrial combustion and processes (IND), gas venting and flaring (FLR), solvent production and use (SLV), transport (TRA), international shipping (SHP), agriculture (AGR), open burning of agricultural waste (AWB), residential combustion (DOM) and waste (WST). Fire emissions, including large-scale biomass burning and savannah burning, were added from SSP2-CMIP6 (projections) and van Marle et al. (2017) subtracting the AWB emissions to avoid double counting. Also natural emissions from dust and sea salt (SS) are considered while international aviation and biogenic emissions are not included.

The **current legislation baseline (CLE)** scenario assumes the implementation of the existing legislation (committed before 2018). It is based on statistical data for a series of drivers including fuel consumption (until 2015) from IEA (International Energy Agency), agriculture from FAO (UN Food and Agriculture Organisation) and IFA (International Fertilizer Organization), and industry, waste, shipping, etc., from other sources (IEA, 2018; Klimont et al., in preparation). Concerning the WB, the CLE assumes a certain degree of alignment with the *EU acquis*. This scenario considers the Energy Community Treaty (all the WB countries are parties) which imposes the implementation of the EU Large Combustion Plants (LCP) Directive (European Union, 2001) by 2018. In addition, CLE assumes the implementation of the EU legislation for the

transport sector with a 10-years delay compared to the EU27. By contrast, the CLE does not include all the measures needed for implementing the *EU acquis* in the WB, because the WB legislation in this field is still under development and the progress varies considerably among countries (Banja et al., 2020). In particular, this scenario does not include significant measures to abate emissions from agriculture nor from wood burning in the residential sector, an important source of wintertime air pollution.

To assess the impact of "no action" on the one hand and the benefit that could be achieved by implementing sustainable policies, on the other hand, a set of marker scenarios were analysed (Table 1). The case where no new policies are introduced beyond the years 2015–2018 is depicted in the **NFC (no further control) scenarios**. The NFC includes two scenarios: the NFC base which relies on the same activity drivers as the CLE (NPS, new policy scenario) and the NFC CPS (current energy policies). By comparison, the **maximum feasible reduction (MFR) scenarios** assume a stringent policy from 2020 onwards. The MFR base relies on the same drivers as the CLE while MFR SDS relies on the IEA sustainable development scenario. The MFR scenarios sketch a spectre of emission scenarios for a first estimate of the environmental benefits arising from a full alignment with the *EU acquis*, including the Green Agenda for the Western Balkans, and going beyond.

The population trends adopted for this study are taken from the Shared Socioeconomic Pathways (SSP) (Riahi et al., 2017; Jones and O'Neill, 2016). In particular, SSP2 ('middle of the road scenario') was chosen for CLE, MFR base and NFC scenarios while SSP1 ('sustainability scenario') was associated with MFR SDS scenario. The population scenarios differ mainly by the population number (5.5 and 9.3 billion in 2050 for SSP1 and SSP2 respectively) and the percentage of people living in densely populated areas. In both scenarios, the proportion residing in higher density areas increases significantly by 2050, but is lower in SSP1 than in SSP2.

In this study, the emission reduction is applied to a source region including the WB plus Croatia and the results are provided in aggregated form for the six WB countries.
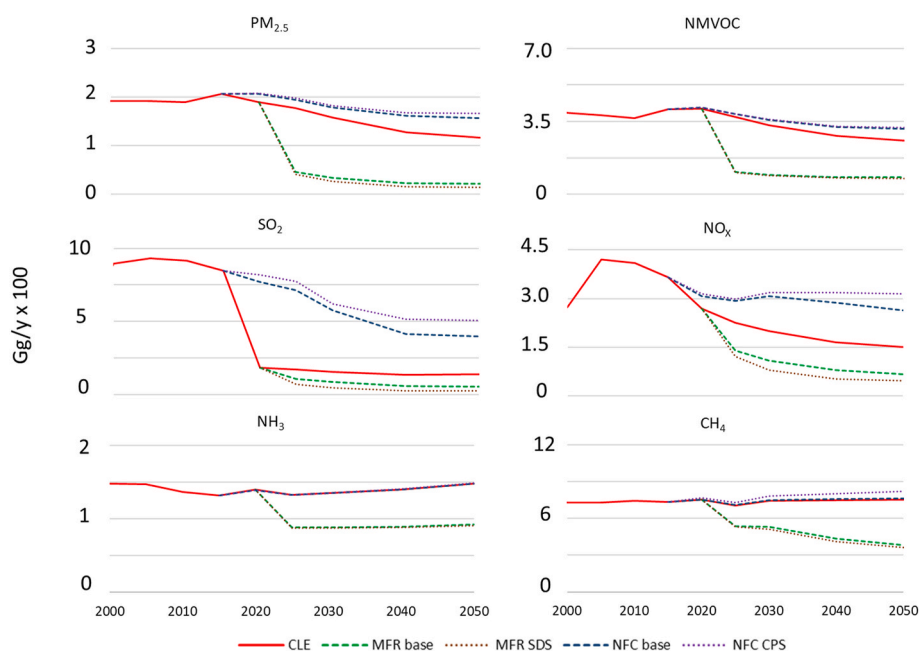

Fig. 1. Past and future trends of $PM_{2.5}$, NOx, NMVOC, SO_2, NOx, NH_3 and CH_4 emissions in the WB as defined in the scenarios used in this study.

3. Results and discussion

3.1. Pollutant emission trends

The trends of $PM_{2.5}$, NMVOC, SO_2, NOx, NH_3 and CH_4 emissions in the WB according to the different scenarios are shown in Fig. 1. NMVOC, NOx and CH_4 are O_3 precursors while NOx, SO_2 and NH_3 are precursors of secondary $PM_{2.5}$. The CLE scenario covers past and future emissions while the NFC and MFR scenarios start from 2020 and 2025, respectively. Between 2000 and 2015, the $PM_{2.5}$, CH_4 and NMVOC emissions remained relatively stable while those of SO_2 and NH_3 decreased slightly. By comparison, NOx emissions grew between 2000 and 2005 and then declined. Such fluctuations have been associated with the recovery of the economies, and consequently of the industrial and transport sector activity, during the late nineties and early 2000s followed by the progressive introduction of abatement measures in the 2010s. In the CLE scenario, $PM_{2.5}$, NMVOC, SO_2 and NOx emissions decline from 2015 onwards with the first two dropping by nearly 40% between 2015 and 2050, and the latter two falling by 84% and 59%, respectively, in the same time window. Such trend is the result of the measures in the power sector, connected to the Energy Community Treaty, and those for the domestic and transport sectors in the longer term. Conversely, NH_3 emissions remain constant and those of CH_4 only increase slightly between 2015 and 2050 since the emissions of these two gases from agriculture are not targeted in the CLE scenario. The MFR scenarios present a dramatic decrease in emissions compared to 2015 for all pollutants, which in 2050 are in the range 40%–88% lower than CLE due to the introduction of best available technologies in the industry, driven by compliance with the EU Industrial Emissions Directive (IED; European Union, 2010), and measures in the energy and residential sectors. In the NFC scenarios, $PM_{2.5}$, NMVOC and SO_2 have steadily downward trends while NOx increases slightly between 2025 and 2030 and subsequently remains relatively stable. For each of these four pollutants, the emissions in the NFC scenarios are higher than those of CLE and in the cases of NOx and SO_2, by a factor of 2 or 3, respectively, due to the absence of LCP Directive provisions and vehicle emission standards. On the contrary, there are little differences between NH_3 and CH_4 emissions in the NFC scenarios and the CLE, indicating very little legislation prior to 2015–2018 concerning these pollutants. Compared to CLE, higher CH_4

emissions in the NFC CPS scenario are driven by absence of the NDCs implementation.

A comparison with some EU neighbour member states (HU, RO, BG and GR) shows that the measures in the CLE tend to align the WB SO_2 and NOx future emissions trends with these countries while those of $PM_{2.5}$ and NMVOC remain at higher levels for the entire time window (Figure S5). By contrast, the drop in WB $PM_{2.5}$ and NMVOC emissions in the MFR scenarios leads to an alignment with the trends in the EU neighbours also for these pollutants.

According to the CLE scenario and the EDGAR 6.0 database (Crippa et al., 2021), the WB total CO_2 emissions increased by 22% between 2000 and 2005 and remained relatively stable until 2015 (Figure S6). The CLE scenario projects the maximum CO_2 emission levels in 2020 (38% higher than 2000) and then a progressive decrease until 2050 when the emissions level off at 9% above 2000 levels.

3.2. Metrics to estimate the exposure to air pollutants in the WB

The temporal evolution of the metrics used to estimate the exposure to ambient air pollutants in the WB is shown in Fig. 2. Between 2000 and 2015, the population-weighted $PM_{2.5}$ concentration for the entire WB region decreased by 2 $\mu g/m^3$ (−14%). In the CLE scenario, the levels of this pollutant decrease by a further 5 $\mu g/m^3$ (−37%) between 2015 and 2050. The implementation of the measures foreseen in the MFR scenarios reduce the population weighted $PM_{2.5}$ by 41%–46% (MFR base and MFR SDS, respectively) in 2050, compared to the CLE scenario. Conversely, failing to implement additional abatement strategies after 2018 gives an increase in population weighted $PM_{2.5}$ of 28%–40% (NFC base; NFC CPS) compared to the CLE scenario in 2050. The reduction of weighted $PM_{2.5}$ between 2015 and 2050 despite 'no further control' is due to the penetration of more efficient technologies in e.g. car fleets and industrial processes.

Similarly, the seasonal daily maximum 8 h average O_3 (SDMA8h) decreased by 1 ppb (2%) between 2000 and 2015. In the CLE scenario, the levels of this pollutant decrease by another 2 ppb (4%) between 2015 and 2050. The MFR scenarios lead to an exposure decrease of 14%–18% (base and SDS, respectively) compared to CLE in 2050. On the contrary, the NFC scenarios foresee a higher exposure (4%–8%) compared to the CLE by 2050.
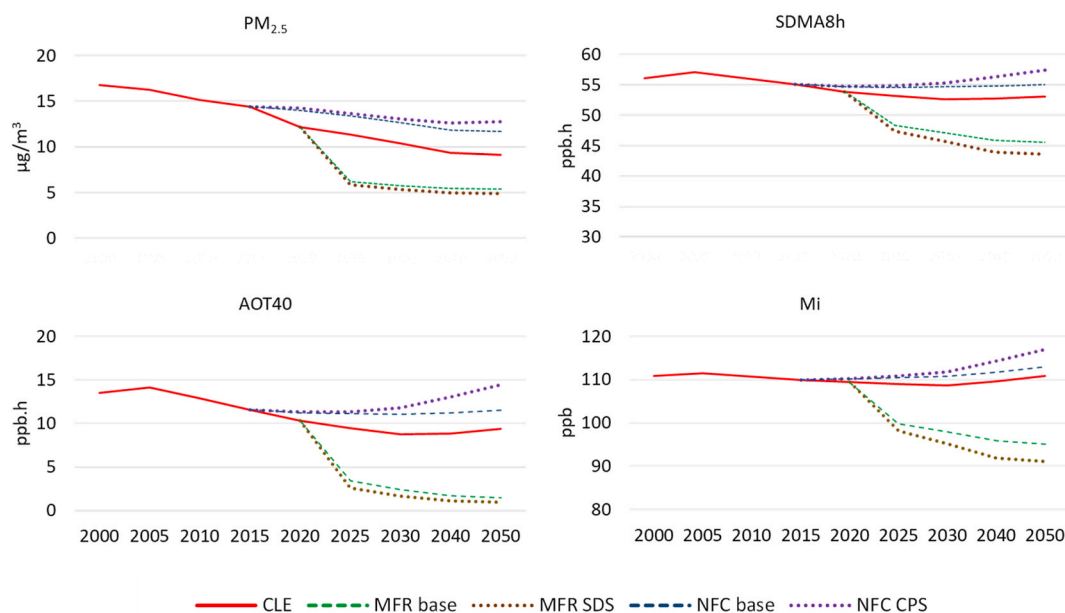

Fig. 2. Past and future trends of population-weighted $PM_{2.5}$ and seasonal daily maximum 8 h average O_3 metrics (SDMA8h) and crop exposure metrics (AOT40, Mi) in the WB. Mi is a combination of M7 and M12 depending on the crop.
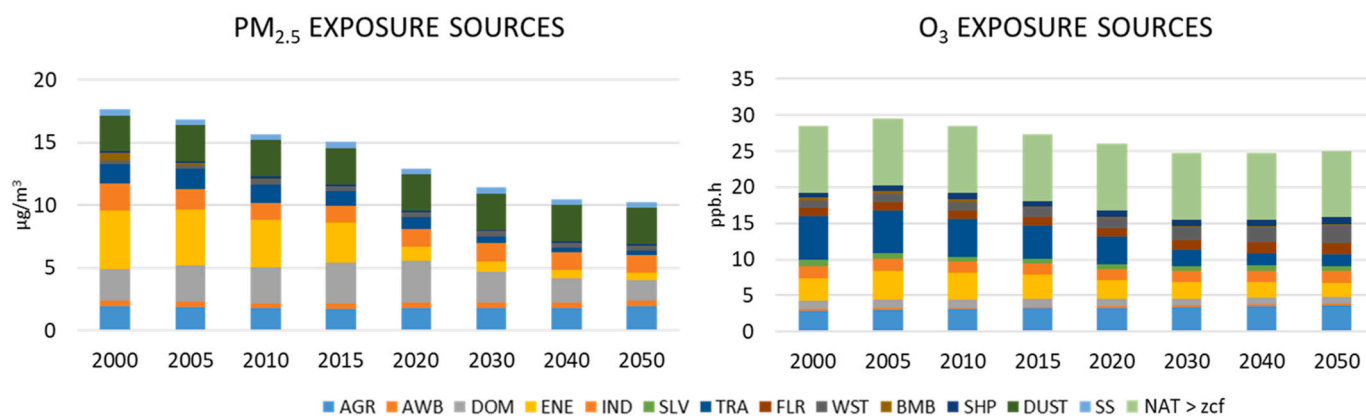
Fig. 3. Past and future trends of the source impacts on $PM_{2.5}$ and O_3 exposure in the CLE scenario. Aviation and secondary organic aerosol are not considered.

The AOT40 O_3 crop exposure metric used to estimate the crop yield losses follows a similar trend as SDMA8h in the CLE scenario with the difference that it experiences a steeper reduction. It dropped by 14% between 2000 and 2015 and a further 19% decrease is foreseen between 2015 and 2050. On the contrary, the Mi only slightly decreased between 2000 and 2015 (1%) and follows a similar trend after 2015 with the exception of 2050 where there is a slight increase. Noting that AOT40 is a threshold metric which emphasises peak values, while the Mi metric represents rather mean values, the shown trends suggest that O_3 peak values are more sensitive to emission changes than the mean daytime O_3 exposure.

3.3. Source attribution of exposure

The impact of pollution sources on exposure metrics and consequently on the estimated health impacts is depicted in Fig. 3. In CLE, the main anthropogenic pollution source leading to $PM_{2.5}$ exposure in 2000 is ENE (26%) followed by DOM, AGR and IND. Between 2000 and 2050 the share of anthropogenic sources progressively decreases leading to an increase in the relative impact of natural components (DUST and SS). Such downward trend is mainly driven by the drop in ENE and TRA impacts (−87% and −75%, respectively). By comparison, AGR, AWB and WST impacts remain stable or increase slightly over the considered time window leading to a sizeable increase in their shares in 2050 compared to 2000. DOM is the only source with an increasing impact from 2000 to 2015 and a subsequent reduction between 2020 and 2050.

The sum of anthropogenic sources contribution to O_3 exposure is only a fraction of total O_3, due to the contribution from biogenic NMVOC and methane, NOx from lightning and biological decay, and stratospheric intrusion. In our reduced modelling framework, this non-anthropogenic portion of O_3 (labelled NAT) is fixed and does not change with changing (anthropogenic) emissions. NAT is estimated by subtracting the sum of the anthropogenic source contributions from the total O_3 concentration, and generally exceeds the zero-risk threshold *zcf* of 29.1 ppb. For the evaluation of source contributions to the health impact we therefore only consider the NAT fraction above *zcf* (NAT > zcf). This fraction is the main source of O_3 exposure in CLE, with a share growing from 32% in 2000 to 37% in 2050 (Fig. 3). TRA, ENE and AGR are the main anthropogenic sources responsible for 21%, 11% and 10% of the total O_3 exposure in 2000. Like $PM_{2.5}$, the impacts of ENE and TRA drop considerably in the observed time window (−75% and −35%, respectively). However, such reduction is offset by the increase in WST, AGR and SHP impacts over the same period (125%, 25% and 36%, respectively).

The sources associated with higher $PM_{2.5}$ exposure levels in the NFC scenarios compared to CLE are TRA, ENE and SHP, which in 2050 are between 80% and 200% higher while TRA is the main source causing higher O_3 exposure in the NFC scenarios (+115 to +176% in 2050) followed by ENE and SHP (+30% in the same year). By comparison, the lower $PM_{2.5}$ and O_3 exposure in MFR scenarios compared to CLE is more homogeneously distributed among all the anthropogenic sources (70%–95% reduction) with the exception of AGR (only 35% $PM_{2.5}$ exposure reduction) and TRA (only 30% O_3 exposure reduction in MFR BASE).

3.4. Mortality

Fig. 4 shows the trends in mortality rate in the WB for the CLE scenario associated with the six $PM_{2.5}$-related causes of death (COD) and O_3-related COPD according to the global burden of disease (GBD 2017) and Turner (TUR) methodologies.

The WB average $PM_{2.5}$ mortality rate increased slightly from 2000 to 2015 (+12%) while an overall decrease is projected between 2015 and 2050 (−10%), despite an uptick between 2040 and 2050. The mortality associated with O_3 is one order of magnitude lower than that due to $PM_{2.5}$, however, the former increased more than the latter between 2000 and 2015, 23%–30%, depending on the exposure impact method.
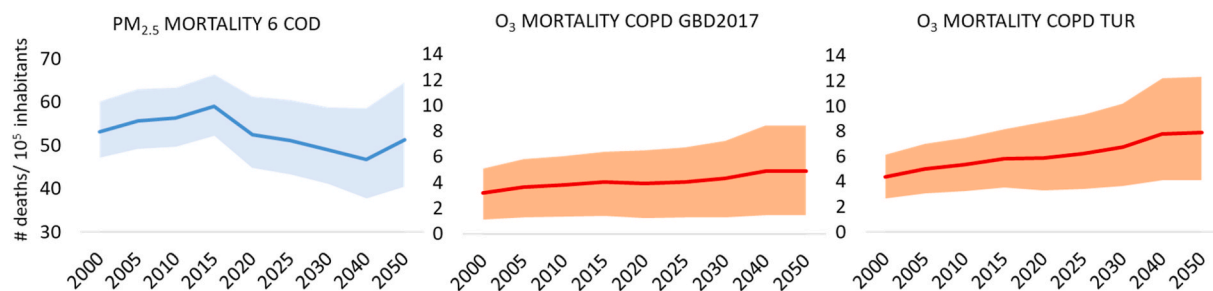

Fig. 4. Past and future trends of mortality (per 100,000 inhabitants) in the CLE scenario associated with six causes of death for $PM_{2.5}$ and Chronic Obstructive Pulmonary Disease for O_3 in the WB with 95% confidence interval (GBD 2017: Global Burden of Disease methodology 2017, Stanaway et al., 2018; TUR: Turner et al., 2016 methodology).
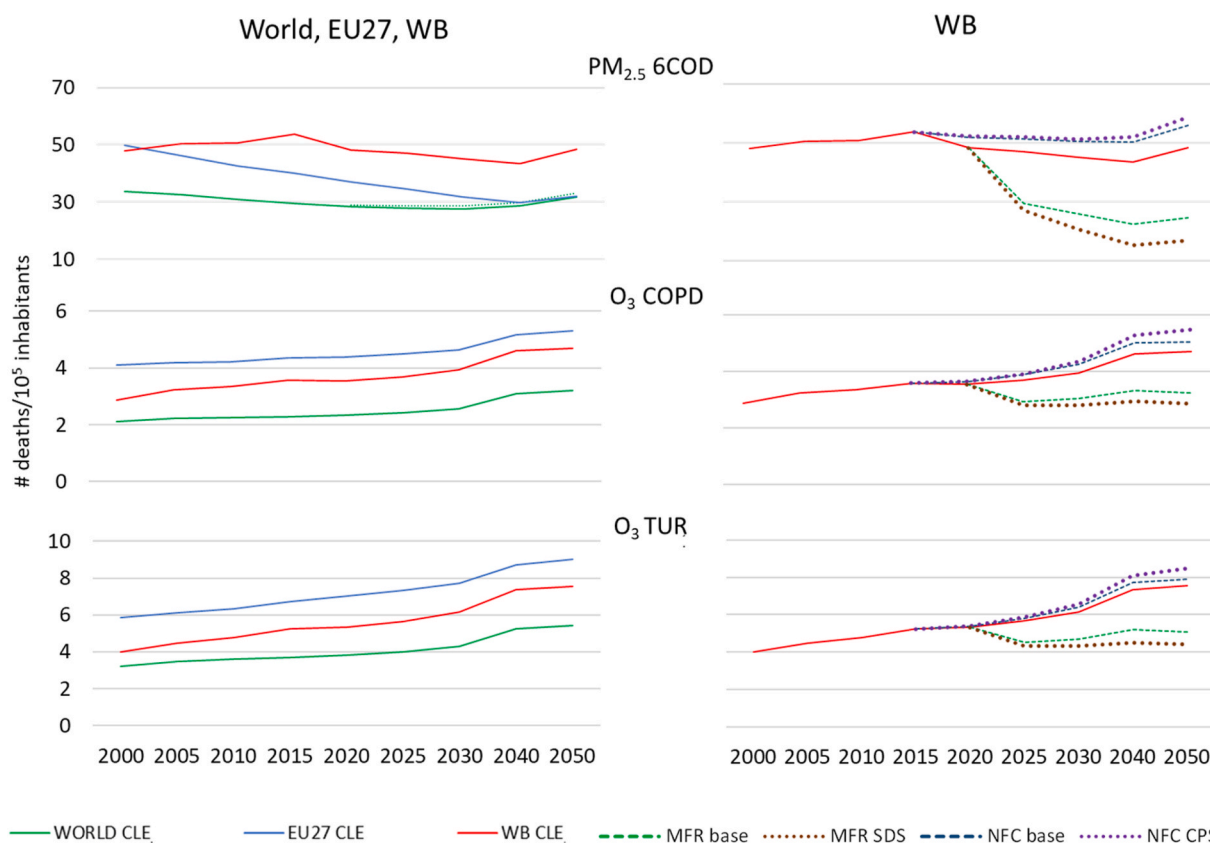
Fig. 5. Past and future scenario trends of average mortality rate (per 100,000 inhabitants) associated with PM$_{2.5}$ six causes of death (COD) and O$_3$ COPD according to global burden of disease (GBD 2017) and Turner (TUR) methodologies in the WB compared with EU27 and global (left) and comparison between scenarios (right).

Moreover, under the CLE base scenario assumptions, O$_3$-related mortality grows between 2015 and 2050 (31%–44%) despite the (slightly) decreasing trend in the O$_3$ exposure metrics. The mortality trends associated with these two pollutants are explained by the interplay of different factors: (a) the trend of the exposure metrics, (b) the evolution of population age structure in the WB, and (c) the different CODs associated with each pollutant. In Fig. 2 it is shown that the exposure metrics are projected to decrease in time which should drive the mortality associated with air pollution downwards. However, the projection of the WB population age structure shows a growing proportion of the population aged over 65 (Figure S7). Since the mortality attributed to air pollution is a fraction of the total mortality and the population ageing leads to higher mortality, also the mortality attributable to air pollution tends to grow. Finally, the trends in the mortality of these pollutants also depend on those of the all-risk mortality for the relevant COD (Figure S8). Since the most important CODs associated with PM$_{2.5}$ (IHD and stroke) decrease between 2015 and 2050, this factor contributes to pull down the mortality attributable to this pollutant. On the contrary, the mortality rate due to COPD, the only COD associated with O$_3$, grows steadily over whole time window contributing to the upward trend of the mortality related to this pollutant.

In Fig. 5 we compare the CLE trends of PM$_{2.5}$ and O$_3$-related country

average mortality rates in the WB with those in EU27 and the globe (left). In 2000, the PM$_{2.5}$ mortality in the EU27 exceeded the WB and the rest of the World. However, by 2015, the WB mortality was 30% and 70% higher than the EU27 and the World average mortality for the same cause, respectively, while in 2050 the EU27 is aligned with the World average mortality and the WB is 60% higher than both of them. Such decoupling between the EU and the WB trends is likely associated with the slower decrease in WB PM$_{2.5}$ emissions compared to EU countries in the CLE scenario where the alignment with the *EU acquis* is limited to some sectors while measures tackling domestic heating and agricultural emissions are missing. As for O$_3$ mortality rate, the EU27 presents the highest average values compared to the WB and the global averages and the temporal trends (growing) for the three geographic aggregations are comparable.

On the right side of Fig. 5, the mortality in the CLE scenario is compared with the other scenarios. The implementation of MFR in the WB leads to a decrease in PM$_{2.5}$ mortality of 49%–65% (base and SDS, respectively) in 2050. Failing to implement further measures after 2018 (NFC) leads to a PM$_{2.5}$ mortality increase of 16%–21% in 2050 compared to the CLE. The same analysis for the O$_3$-related mortality leads to a decrease of 31%–42% 2050 compared to the CLE for the MFR scenarios and an increase in mortality of 5%–17% in 2050 for the

Table 2
Deaths attributable to the individual PM$_{2.5}$ causes of mortality (CLE base) in the Western Balkans, expressed as percentage of the annual total PM$_{2.5}$-related mortality.

	2000	2005	2010	2015	2020	2025	2030	2040	2050
COPD	9	9	10	10	10	10	11	12	11
LC	9	10	10	10	10	10	10	10	9
LRI	4	3	3	3	3	3	3	4	3
DM	6	8	10	11	11	11	11	11	10
IHD	42	40	39	39	42	42	41	41	44
STROKE	30	29	28	27	24	24	24	22	24

Table 3
Variations of transboundary air pollution health impacts (mortality) in the WB.

Time window	2000–2015	2015–2050	2050							
Parameter	DELTA 2000–2015	DELTA 2015–2050	DELTA to CLE-base							
ds	CLE-base	CLE-base	MFR-base		MFR-SDS		NFC-NPS		NFC-CPS	
Units	# deaths	# deaths	# deaths	%	# deaths	%	# deaths	%	# deaths	%
			$PM_{2.5}$							
Domestic	−104	−2212	−3297	−39	−5372	−64	1044	12	1394	17
Export	91	−864	−2263	−27	−2558	−30	1301	16	1752	21
Import	948	−915	−1565	−19	−2922	−35	370	4	640	8
ratio Δexp/Δimp	0.9	1.4		0.9		3.5		2.7		
ratio Δdom/Δimp	2.4	2.1		1.8		2.8		2.2		
			O_3							
Domestic	−71	8	−25	−3	−31	−4	27	4	44	6
Export	−226	998	−237	−31	−261	−34	87	11	151	20
Import	215	3	−226	−30	−284	−37	36	5	97	13
ratio Δexp/Δimp	338	1.0		0.9		2.4		1.6		
ratio Δdom/Δimp	2.6	0.1		0.1		0.8		0.5		

Note 1: domestic: emission and impact in WB, export: emission in WB and impact elsewhere, import: emission elsewhere and impact in WB. Note 2: when import and export or domestic and import are of opposite signs their ratio is not reported.

NFC scenarios.

Table 2 shows a more detailed picture of the six CODs associated with $PM_{2.5}$. IHD and stroke represent on average two thirds of all the $PM_{2.5}$ mortality cases, the share of COPD, LC and DM is approximately 10% of the cases each while LRI is the COD with the lowest incidence (4% on average). The IHD share is relatively stable along the study timeframe while stroke shows a decreasing trend between 2015 and 2050. On the contrary, DM, which represents both types of diabetes mellitus, shows an upward trend between 2000 and 2015 and, due to the lack of projections, a constant value is assumed from 2015 onwards.

The COD trends indicate that the increase of 10% in $PM_{2.5}$ mortality in 2050 compared to 2040 seen in all three geographical aggregations (WB, EU7 and World, Fig. 4), is associated with an increase in deaths due to cerebrovascular diseases (IHD and stroke).

3.5. Transboundary pollution and health impacts

In this section, the contribution of domestic, exported and imported fractions to the overall exposure to $PM_{2.5}$ and O_3 in the WB region and the associated mortality (# deaths) is assessed. Table 3 (left) shows the changes in the domestic and transboundary impacts for the CLE scenario in 2015 relative to 2000 and in 2050 relative to 2015.

Between 2000 and 2015 there was a reduction of deaths caused by WB $PM_{2.5}$ emissions in the WB (domestic), associated with a population decline (−1%) in this area during this interval, while those caused by WB emissions in other regions (export) increased (EU27 and global populations increased by 5% and 20%, respectively in the same interval). In addition, despite the population decrease, there was an increase of deaths in WB caused by $PM_{2.5}$ emission from other regions (import). The comparison of the changes in mortality caused by transboundary pollution in this period clearly indicates a lower impact of the WB on the surrounding areas compared to the impact that surrounding areas had on the WB. This is associated with transboundary contributions from neighbour countries such as RO, HU, BG and Ukraine, which are more populated and industrialised compared to the WB. In the same period, O_3-related mortality due to WB emissions showed a reduction in both the exported and the domestic fractions. However, like $PM_{2.5}$, the imported O_3-related mortality increased, most likely due to the increasing trend of the COPD all-risk mortality as discussed above (Figure S8). Overall, in the period 2000–2015 changes in "transboundary mortality" (i.e. import and export) are greater than those in WB domestic mortality. Between 2015 and 2050, $PM_{2.5}$-related mortality in CLE is projected to decrease and unlike the previous period, the drop in the domestic component dominates the transboundary component, emphasising the importance of implementing the already announced abatement measures in the WB. By comparison, in this period the O_3-related mortality would shift to a steadily growing trend in the CLE scenario, most likely due to the effect of the abovementioned growing trend in the COPD all-risk mortality. In addition, because of the secondary nature of O_3 and its longer atmospheric lifetime compared to $PM_{2.5}$, the transboundary (export) mortality is strongly dominant suggesting that additional co-ordinated abatement efforts across countries and regions are needed for this pollutant.

The right side of Table 3 shows the mortality changes in the MFR and NFC scenarios with respect to CLE in 2050. As expected, the MFR scenarios produce fewer deaths with respect to CLE case, while the NFC ones produce higher mortality rates relative to the baseline.

The relationship between domestic and imported $PM_{2.5}$-related mortality does not change significantly between MFR and NFC scenarios. However, the ratio exported/imported is considerably higher in the NFC scenarios with respect to the MFR scenarios suggesting that lack of action in the WB would increase the impact of the WB on neighbouring countries. Turning to the O_3-related mortality, there is an equilibrium between exported and imported in the MFR scenarios, while exported mortality dominates the NFC scenarios, leading to the same conclusion about the impact of no action in the WB as $PM_{2.5}$. Conversely,
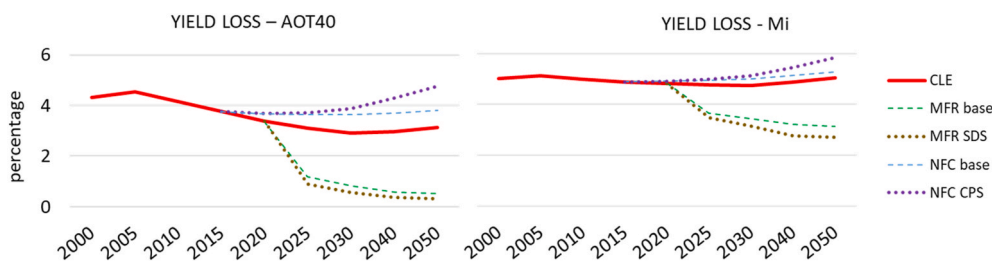

Fig. 6. Past and future scenario trends of crop relative yield loss associated with O_3 in the WB estimated using AOT40 and Mi O_3 exposure metrics.

domestic O_3-related mortality is always lower than transboundary mortality confirming that the regional background predominates for this pollutant.

3.6. Crop yield loss

In Fig. 6, the WB crop relative yield losses (RYL) estimated with two different metrics (AOT40 and Mi) for the CLE, MFR and NFC scenarios are shown. In 2000, the total RYL of the four crops studied (wheat, maize, soybean and rice) attributable to O_3 in the WB was 4%–5%, depending on the O_3 metrics. The yield losses in the CLE scenario follow a downward trend (the slope is steeper for AOT40) reaching minimum values in 2030 (at 3%–5% for AOT40 and Mi, respectively) with a slight trend inversion in 2040.

In general, the projected RYLs obtained with the Mi metric are higher than those derived with the AOT40 while the latter shows a steeper downward trend. The differences between the two metrics are partly due to the AOT40 being a threshold which makes it more difficult to be modelled with linear relationships. In addition, AOT40 mostly represents the maximum exposure levels while the Mi reflects the averages and, as described below, each crop seems to show different sensitiveness depending on the used metric.

According to the CLE scenario, in 2015 RYLs remained stable or decreased up to 13% relative to 2000 (depending on the metrics) and are foreseen to remain stable or decrease at most 17% between 2015 and 2050. The implementation of the measures considered under the MFR scenarios leads to an almost complete elimination of the O_3 impact with 83%–90% reduction in 2050 compared to the CLE according to the AOT40 estimations. By comparison, AOT40 based RYLs in the NFC scenarios lead to an increase of 22%–52% in 2050 relative to the CLE. The relative temporal trends are similar when using Mi, however, the reductions in the MFR scenarios with respect to the CLE are lower, in the range 38%–46% for 2050. On the other hand, according to this metrics the increase in RYLs due to the lack of action (NFC scenarios) in 2050 are

in the range 5%–16%.

The trends of the absolute yield losses in the WB computed with AOT40 and Mi metrics according to the CLE scenario for each of the considered crops are reported in Figure S9. Wheat and maize are the main crops produced in the WB and, consequently, are those with the highest absolute losses (while soybean and rice have a marginal share of both production and losses). Wheat suffers the highest absolute yield losses according to AOT40 while Mi attributes the highest damage to maize.

3.7. Climate metrics

The effect of the air pollutant emissions with an impact on the radiative balance of the atmosphere, also called short-lived climate forcers (SLCF; IPCC, 2021), was evaluated in order to assess the co-benefits between air quality and climate policies. For this purpose, we used the global warming potential (GWP), an index of the total energy added to a climate system by a component relative to that of CO_2 which is often referred to as "CO_2 equivalent emissions" (IPCC, 2021).

For each SLCF (p) and time horizon (h), the CO_2 equivalent emissions based on GWP were obtained from:

$$CO_{2eq,p} = EM_p \times GWP_{h,p}$$

The GWP can be integrated over different time horizons. Policy analysis of climate impacts are generally based on 100-year GWP (GWP100), which gives greater weight to the long-lived climate forcers such as CO_2 and N_2O. Considering that this analysis is based on projections for SLCFs until 2050, we also discuss the GWP integrated over 20 years (GWP20).

In Fig. 7 the trends of total CO_2 equivalent emission changes, relative to year 2000, corresponding to the GWP100 and GWP20 for all the scenarios are shown on the left while the breakdown of the GWP20 by precursor for three selected scenarios (CLE, MFR SDS and NFC CPS) are displayed on the right.
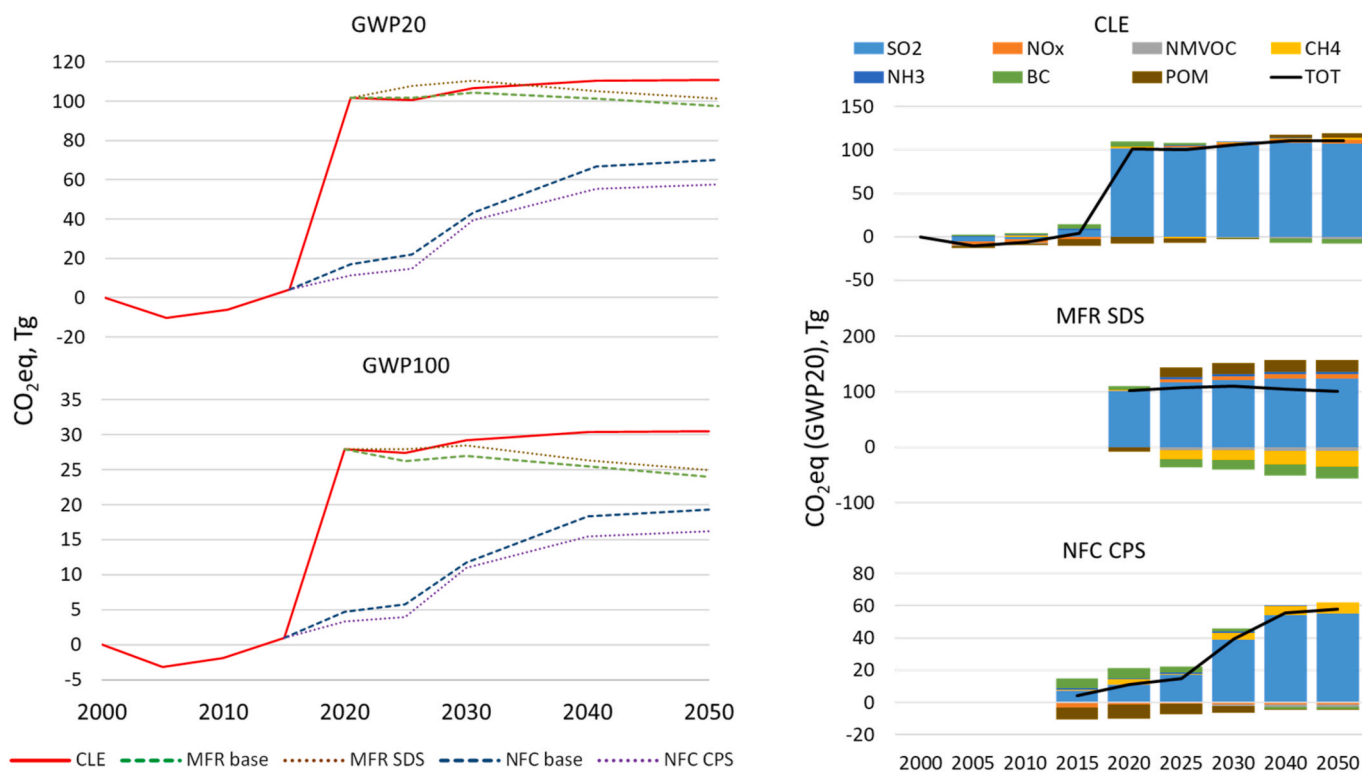

Fig. 7. Trend of CO_2 equivalent SLCF emissions in the WB corresponding to the GWP computed for 20 and 100 years (reference year 2000). On the right is reported the breakdown of the GWP20 for the single precursors in three selected scenarios.

Due to their short lifetime compared to CO_2, the climate impacts of SLCF are more than a factor 3 greater in the short term. Consequently, despite the comparable trends for these two time horizons in Fig. 7, the SLCF CO_2eq emissions are higher in GWP20 compared to GWP100. For reference, the fossil CO_2 emissions have increased by 21 Tg between 2000 and 2020 in the WB, while in the EU27 they decreased by 955 Tg over the same period (Crippa et al., 2021).

The CO_2eq emissions of the SCLF in the WB decreased after 2000 and returned to the 2000 levels in 2015. A dramatic increase is observed in the CLE scenario between 2015 and 2020 and then the levels continue to grow slightly until 2050. The CO_2eq in the MFR scenarios are higher than those of the CLE in 2025 and subsequently decrease progressively until 2050 when they reach a level 5%–8% lower than the CLE. By comparison, the NFC scenarios present CO_2eq considerably lower than the CLE and since 2015 grow gradually showing a tendency to converge with the MFR in 2040–2050 even though levels remain lower than the latter scenario. The breakdown of the total GWP20 CO_2eq emissions by single precursor contribution in Fig. 7 (right) indicates that the described trends are mainly determined by the changes in SO_2 emissions. The low between 2000 and 2015 matches the maximum SO_2 emissions rates while the strong reduction of such pollutant emissions between 2015 and 2020 in the CLE (Fig. 1) corresponds with the dramatic increase in the CO_2eq emissions in this time window. The cooling (negative CO_2eq) effect of the BC and CH_4 emission reductions in the MFR counterbalance the warming effect of the SO_2 reductions eventually leading to a downward trend in these scenarios. On the other hand, the lower and progressive SO_2 reductions in the NFC scenarios determine a more gradual increase in the warming effect.

The results of this analysis demonstrate that the CLE scenario, which includes the Paris Agreement NDCs, is the one with the highest SLCF impacts on climate over the studied 50-year time frame, no matter what is the time horizon used to compute the CO_2eq emissions. However, the implementation of the MFR scenarios would contribute to offset in part the warming impact of the CLE scenario. The NFC scenarios are those with the lower warming impact in the short term, likely due to the limited SO_2 emission reduction, even though such impacts tend to converge with those of the MFR scenarios in the longer term.

4. Comparison with previous work and limitations of the study

The $PM_{2.5}$-related deaths estimated in the present study for 2015 were compared with those estimated for the closest available year (2016) in other studies (UNEP, 2019; EEA, 2019; World Bank, 2019a; World Bank, 2019b) and the results are summarised in Figure S10. The proportion between the mortality in the single countries is similar in the different studies. The TM5-FASST estimations lie at the lower end of the mortalities range reported in the considered studies suggesting that the output of our present work can be considered as conservative estimations. In Figure S10 (right) the mortality attributable to O_3 estimated in the present study for 2015 with the GBD and Turner approaches is compared with those estimated for 2016 with the HRAPIE approach (EEA, 2019). The relationship between TM5-FASST results and those reported by the EEA change from country to country, however, the WB overall figures are coherent since the EEA estimations fall in between the range determined by the two approaches used in the present study. The apportionment of the source impacts on $PM_{2.5}$ exposure obtained in this study for five Western Balkans (excluding Kosovo) is comparable with the one proposed by the Health Effects Institute (HEI, McDuffie et al., 2021). DOM and IND impacts are 4%–5% higher in TM5-FASST, respectively, while ENE is 5% higher in the results reported by HEI (Figure S11). All the other source impacts are within 2 percentage points.

The variability between studies may be attributed either to differences in the input data (population and concentration based exposure indicators) or to the concentration-response function used to estimate mortality. The population used for the present study are derived from

scenarios (section 2.2) while the levels of pollutants are discussed in section 3.2. In the UNEP-WHO study, the exposure was estimated with the model DIMAQ and the Air Q+ tool (World Health Organisation, 2020) which is based on a log-linear exposure function for estimating $PM_{2.5}$ impacts on all-(natural) cause mortality and on the GBD IER functions for IHD and cerebrovascular deaths. By comparison, in the present study the estimations are based the IER functions of the GBD2017 for every relevant COD (section 2.1). Also the cut off level for $PM_{2.5}$ mortality varies between studies. In the UNEP-WHO study it is 10 μg/m^3, TM5-FASST uses 2.4–5.9 μg/m^3 (depending on the COD) while there is no cut off in the HRAPIE approach adopted in the EEA study.

One of the limitations of the study is that the NO_2 related health impacts are not considered preventing the estimation of the overall impact of air pollution on health. In addition, this study is based on modelled concentrations which are affected by the patchy and inaccurate emission data available for the WB (Belis et al., 2019; Banja et al., 2020). This leads to estimations that are lower than those obtained by a combination of modelled and measured concentrations (e.g. DIMAQ). Such impact, however, is evident only for $PM_{2.5}$ while O_3 estimations a less affected by local emissions. Moreover, the focus of this study is on the variations between scenarios compared to the base case over the entire region. Therefore, the consistency of the methodology used in the different runs and the model capacity to detect trends and differences between scenarios are the key features of the adopted approach while the absolute concentration of pollutants and their local gradients have a relatively small influence on this analysis.

5. Conclusions

This study focuses on the Western Balkans, an area of low-medium income countries, with a critical domestic and transboundary air pollution situation, which are in a phase of deep transformation due to their perspective of becoming European Union members. This case study represents an example of how the support of a developed area with high environmental standards can create the conditions for an enhanced sustainability long-term perspective in nearby less developed regions.

The scenario analysis carried out with TM5-FASST delivered a range of projections for key sustainability indicators such as the impacts of air quality on health and climate and also an indicator for a key economic variable like the agricultural production. In the absence of specific policy targets for the entire WB region, in the present study the ECLIPSE V6b global emission scenarios, developed with a consolidated methodology, were used to ensure the robustness of the results and their comparability with similar studies in other regions of Europe and the World. In addition, ECLIPSE V6b scenarios made it possible to analyse projections over some decades which is essential to understand the long-term implications of the policies and their compliance with long-term targets like those established in the SDGs and the EU-GD, and in international conventions such as the Air Convention, the Paris agreement and the Energy Community.

The results of the present study confirm that the implementation of the currently adopted policies in the WB (CLE) are likely stabilising or slightly reducing the $PM_{2.5}$ impact in relation to health and the one of O_3 on agriculture productivity in the coming decades, while the impact of O_3 on health will likely increase. Such policies are effective in abating the projected impact of energy production and transport emissions on both pollutants and of residential combustion on $PM_{2.5}$. However, current policies have little effect on agriculture, waste management and other minor sources which impact is projected to remain stable or increase. In addition, a comparative analysis showed that the baseline projected mortality in the WB present a lower downward slope for $PM_{2.5}$ and a steeper increase for O_3 compared to the EU27.

The MFR scenarios provide a reference of the maximum benefits that could be obtained with ambitious policies that address all the relevant anthropogenic emission sectors without considering costs limitations. On the other hand, the NFC scenarios, confirm that the lack of policy

implementation would lead to a measurable worsening of the impacts on health and crop yields compared to the baseline mainly due to the increased role of transport, energy production and international shipping. Moreover, the TM5-FASST estimate of the transboundary impacts showed that lack of action might cause a 20% increase of mortality associated with $PM_{2.5}$ and O_3 in neighbouring countries due to WB emissions, suggesting the importance of coordinated abatement efforts across regions. The analysis also concludes that currently planned air quality policies would lead to a considerable increase in the warming impact of the WB SLCF emissions and that such situation could be mitigated by measures aiming to meet both the Paris Agreement target of holding global average temperature below 2 °C and the energy-related SDGs.

The Green Agenda for the WB is aligned with the principles of the EU-Green Deal. Since the specific measures related to the WB Green Agenda are still under definition, the CLE and MFR scenarios presented in this study can be considered as a first approximation of the range of impacts that could be expected from the measures outlined therein. The CLE depicts a partial implementation of the *EU acquis* while the MFR describes a situation beyond a full implementation of the *EU acquis* including the abovementioned Green Agenda. More specific analysis would be possible when quantitative policy targets and deadlines for this region are defined. In addition, a continued improvement in the reporting of WB pollutants' emissions is essential to support the policy design and evaluation.

Author statement

Claudio A. Belis: Conceptualization, Formal analysis, Visualization, Writing – original draft. **Rita Van Dingenen**: Investigation, Methodology, Software, Formal analysis, Writing – review & editing. **Zbigniew Klimont**: Data curation, Investigation, Writing – review & editing. **Frank Dentener**: Writing – review & editing

Declaration of competing interest

The authors declare that they have no known competing financial interests or personal relationships that could have appeared to influence the work reported in this paper.

Acknowledgements

Appendix A. Supplementary data

Supplementary data related to this article can be found at https://doi.org/10.1016/j.jenvman.2022.115738.

References

Amann, M., Bertok, I., Borken-Kleefeld, J., Cofala, J., Heyes, C., Höglund-Isaksson, L., Klimont, Z., Nguyen, B., Posch, M., Rafaj, P., Sander, R., Schöpp, W., Wagner, F., Winiwarter, W., 2011. Cost-effective control of air quality and greenhouse gases in Europe: modeling and policy applications. Environ. Model. Software 26, 1489–1501. https://doi.org/10.1016/j.envsoft.2011.07.012.

Avnery, S., Mauzerall, D.L., Liu, J., Horowitz, L.W., 2011. Global crop yield reductions due to surface ozone exposure: 1. Year 2000 crop production losses and economic damage. Atmos. Environ. 45, 2284–2296. https://doi.org/10.1016/j.atmosenv.2010.11.045.

Banja, M., Đukanović, G., Belis, C.A., 2020. Status of Air Pollutants and Greenhouse Gases in the Western Balkans: Benchmarking the Accession Process Progress on Environment. Publications Office of the European Union, Luxembourg, ISBN 978-92-76-16860-7. https://doi.org/10.2760/48321. EUR 30113 ENJRC118679.

World Bank, 2019b. Regional AQM western Balkans. Air Quality Management in North Macedonia, p. 110. Report No: AUS0001228.

World Bank, 2019a. Regional AQM western Balkans. Air Quality Management in Bosnia and Herzegovina, p. 99. Report No: AUS0001227.

Belis, A.C., et al., 2019. Urban pollution in the Danube and Western Balkans regions: the impact of major PM2.5 sources. Environmental International Journal 133, 105158. https://doi.org/10.1016/j.envint.2019.105158.

Belis, C.A., Pernigotti, D., Pirovano, G., Favez, O., Jaffrezo, J.L., Kuenen, J., Denier van Der Gon, H., Reizer, M., Riffault, V., Alleman, L.Y., Almeida, M., Amato, F., Angyal, A., Argyropoulos, G., Bande, S., Beslic, I., Besombes, J.L., Bove, M.C., Brotto, P., Calori, G., Cesari, D., Colombi, C., Contini, D., De Gennaro, G., Di Gilio, A., Diapouli, E., El Haddad, I., Elbern, H., Eleftheriadis, K., Ferreira, J., Vivanco, M.G., Gilardoni, S., Golly, B., Hellebust, S., Hopke, P.K., Izadmanesh, Y., Jorquera, H., Krajsek, K., Kranenburg, R., Lazzeri, P., Lenartz, F., Lucarelli, F., Maciejewska, K., Manders, A., Manousakas, M., Masiol, M., Mircea, M., Mooibroek, D., Nava, S., Oliveira, D., Paglione, M., Pandolfi, M., Perrone, M., Petralia, E., Pietrodangelo, A., Pillon, S., Pokorna, P., Prati, P., Salameh, D., Samara, C., Samek, L., Saraga, D., Sauvage, S., Schaap, M., Scotto, F., Sega, K., Siour, G., Tauler, R., Valli, G., Vecchi, R., Venturini, E., Vestenius, M., Waked, A., Yubero, E., 2020. Evaluation of receptor and chemical transport models for PM10 source apportionment. Atmos. Environ. X 5, 100053. https://doi.org/10.1016/j.aeaoa.2019.100053.

Burnett, R., Cohen, A., 2020. Relative risk functions for estimating excess mortality attributable to outdoor PM2.5 air pollution: evolution and state-of-the-art. Atmosphere 11 (6), 589.

Burnett, R.T., Pope III, C.A., Ezzati, M., Olives, C., Lim, S.S., Mehta, S., Shin, H.H., Singh, G., Hubbell, B., Brauer, M., Anderson, H.R., Smith, K.R., Balmes, J.R., Bruce, N.G., Kan, H., Laden, F., Prüss-Ustün, A., Turner, M.C., Gapstur, S.M., Diver, W.R., Cohen, A., 2014. An integrated risk function for estimating the global burden of disease attributable to ambient fine particulate matter exposure. Environ. Health Perspect. 122, 397–403. https://doi.org/10.1289/ehp.1307049.

Chuwah, C., van Noije, T., van Vuuren, D.P., Stehfest, E., Hazeleger, W., 2015. Global impacts of surface ozone changes on crop yields and land use. Atmos. Environ. 106, 11–23.

Crippa, M., Guizzardi, D., Solazzo, E., Muntean, M., Schaaf, E., Monforti-Ferrario, F., Banja, M., Olivier, J.G.J., Grassi, G., Rossi, S., Vignati, E., 2021. GHG Emissions of All World Countries - 2021 Report. Publications Office of the European Union, Luxembourg, ISBN 978-92-76-41547-3. https://doi.org/10.2760/173513. EUR 30831 ENJRC126363.

Emberson, L., 2020. Effects of ozone on agriculture, forests and grasslands: improving risk assessment methods for O3. Phil. Trans. Math. Phys. Eng. Sci. 378, 20190327.

European Commission (Ec), 2018. A Credible Enlargement Perspective for and Enhanced EU Engagement with the Western Balkans. European Commission. COM(2018) 65 (final).

European Commission (Ec), 2019. The European Green Deal. European Commission. COM(2019) 640(final).

European Commission (Ec), 2020a. Enhancing the Accession Process - A Credible EU Perspective for the Western Balkans. COM(2020) 57 final.

European Commission (Ec), 2020b. Guidelines for the Implementation of the Green Agenda for the Western Balkans. SWD(2020)223 final.

European Environment Agency (Eea), 2019. Air Quality in Europe – 2019 Report. No 10/2019. https://doi.org/10.2800/822355. SBN 978-92-9480-088-6.

European Environment Agency (Eea), 2021. Air Quality in Europe – 2021 Report, ISBN 978-92-9480-403-7. https://doi.org/10.2800/549289. No 15/2021.

European Union (Eu), 2001. Directive 2001/80/EC of the European Parliament and of the Council of 23 October 2001 on the Limitation of Emissions of Certain Pollutants into the Air from Large Combustion Plants.

European Union (Eu), 2010. Directive 2010/75/EU of the European Parliament and of the Council of 24 November 2010 on Industrial Emissions (Integrated Pollution Prevention and Control).

Food and Agriculture Organisation of the United Nations (Fao), 2012. GAEZ latest access. http://www.fao.org/nr/gaez/en/. (Accessed 16 December 2020).

Fuglestvedt, J.S., Shine, K.P., Berntsen, T., Cook, J., Lee, D.S., Stenke, A., Skeie, R.B., Velders, G.J.M., Waitz, I.A., 2010. Transport impacts on atmosphere and climate: Metrics. Atmos. Environ. 44 (37), 4648–4677. https://doi.org/10.1016/j.atmosenv.2009.04.044.

Grulke, N.E., Heath, R.L., 2020. Ozone effects on plants in natural ecosystems. Plant Biol. 22, 12–37.

Health Effects Institute (HEI), 2020. State of Global Air 2020. Health Effects Institute, Boston, MA, pp. 1–28. https://www.healthdata.org/policy-report/state-global-air-2020. (Accessed 26 January 2022). Special Report.

Hollaway, M.J., Arnold, S.R., Challinor, A.J., Emberson, L.D., 2012. Intercontinental trans-boundary contributions to ozone-induced crop yield losses in the Northern Hemisphere. Biogeosciences 9, 271–292.

Intergovernmental Panel on Climate Change (IPCC), 2021. In: Zhai, V.P., Pirani, A., Connors, S.L., Péan, C., Berger, S., Caud, N., Chen, Y., Goldfarb, L., Gomis, M.I., Huang, M., Leitzell, K., Lonnoy, E., Matthews, J.B.R., Maycock, T.K., Waterfield, T., Yelekçi, O., Yu, R., Zhou, B. (Eds.), Climate Change 2021: the Physical Science Basis. Contribution of Working Group I to the Sixth Assessment Report of the Intergovernmental Panel on Climate Change [Masson-Delmotte. Cambridge University Press (Press).

International Energy Agency (IEA), 2018. World Energy Outlook 2018 latest access. https://webstore.iea.org/world-energy-outlook-2018. (Accessed 17 February 2021).

International Institute for Applied Systems Analysis (IIASA), 2021. Global Emission Fields of Air Pollutants and GHG. https://iiasa.ac.at/web/home/research/research Programs/air/ECLIPSEv6.html, latest access. (Accessed 17 February 2021).

Jerrett, M., Burnett, R.T., Arden, P.I., Ito, K., Thurston, G., Krewski, D., Shi, Y., Calle, E., Thun, M., 2009. Long-term ozone exposure and mortality. N. Engl. J. Med. 360, 1085–1095. https://doi.org/10.1056/NEJMoa0803894.

Jones, B., O'Neill, B.C., 2016. Spatially explicit global population scenarios consistent with the shared socioeconomic Pathways. Environ. Res. Lett. 11 (8), 084003 https://doi.org/10.1088/1748-9326/11/8/084003.

Klimont, Z., Höglund-Isaksson, L., Heyes, C., Rafaj, P., Schöpp, W., Cofala, J., Purohit, P., Borken-Kleefeld, J., Kupiainen, K., Kiesewetter, G., Winiwarter, W., Amann, M, Zhao, B., Wang, S.X., Bertok, I., Sander, R. Global Scenarios of Air Pollutants and Methane: 1990-2050. (In preparation).

Klimont, Z., Kupiainen, K., Heyes, C., Purohit, P., Cofala, J., Rafaj, P., Borken-Kleefeld, J., Schöpp, W., 2017. Global anthropogenic emissions of particulate matter including black carbon. Atmos. Chem. Phys. 17, 8681–8723. https://doi.org/10.5194/acp-17-8681-2017.

Krewski, D., Jerrett, M., Burnett, R.T., Ma, R., Hughes, E., Shi, Y., 2009. Extended Follow-Up and Spatial Analysis of the American Cancer Society Study Linking Particulate Air Pollution and Mortality, Research Report. Health Effects Institute, Boston.

Krol, M., Houweling, S., Bregman, B., van den Broek, M., Segers, A., van Velthoven, P., Peters, W., Dentener, F., Bergamaschi, P., 2005. The two-way nested global chemistry-transport zoom model TM5: algorithm and applications. Atmos. Chem. Phys. 5 (2), 417–432. https://doi.org/10.5194/acp-5-417-2005.

McDuffie, E.E., Martin, R.V., Spadaro, J.V., Burnett, R., Smith, S.J., O'Rourke, P., Hammer, M.S., van Donkelaar, A., Bindle, L., Shah, V., Jaeglé, L., Luo, G., Yu, F., Adeniran, J.A., Lin, J., Brauer, M., 2021. Source sector and fuel contributions to ambient PM2.5 and attributable mortality across multiple spatial scales. Nat. Commun. 12, 3594.

Mills, G., Buse, A., Gimeno, B., Bermejo, V., Holland, M., Emberson, L., Pleijel, H., 2007. A synthesis of AOT40-based response functions and critical levels of ozone for agricultural and horticultural crops. Atmos. Environ. 41 (12), 2630–2643. https://doi.org/10.1016/j.atmosenv.2006.11.016.

Monks, P.S., Archibald, A.T., Colette, A., Cooper, O., Coyle, M., Derwent, R., Fowler, D., Granier, C., Law, K.S., Mills, G.E., Stevenson, D.S., Tarasova, O., Thouret, V., von Schneidemesser, E., Sommariva, R., Wild, O., Williams, M.L., 2015. Tropospheric ozone and its precursors from the urban to the global scale from air quality to short-lived climate forcer. Atmos. Chem. Phys. 15, 8889–8973.

Murray, C.J., Ezzati, M., Lopez, A.D., Rodgers, A., Vander Hoorn, S., 2003. Comparative quantification of health risks: conceptual framework and methodological issues. Popul. Health Metrics 1, 1.

Pope III, C.A., Burnett, R.T., Thun, M.J., Calle, E.E., Krewski, D., Ito, K., Thurston, G.D., 2002. Lung cancer, cardiopulmonary mortality, and long-term exposure to fine particulate air pollution. J. Am. Med. Assoc. 287, 1132–1141. https://doi.org/10.1001/jama.287.9.1132.

Riahi, K., van Vuuren, D.P., Kriegler, E., Edmonds, J., O'Neill, B.C., Fujimori, S., Bauer, N., Calvin, K., Dellink, R., Fricko, O., Lutz, W., Popp, A., Cuaresma, J.C., Kc, S., Leimbach, M., Jiang, L., Kram, T., Rao, S., Emmerling, J., Ebi, K., Hasegawa, T., Havlik, P., Humpenöder, F., Da Silva, L.A., Smith, S., Stehfest, E., Bosetti, V., Eom, J., Gernaat, D., Masui, T., Rogelj, J., Strefler, J., Drouet, L., Krey, V., Luderer, G., Harmsen, M., Takahashi, K., Baumstark, L., Doelman, J.C., Kainuma, M., Klimont, Z., Marangoni, G., Lotze-Campen, H., Obersteiner, M., Tabeau, A., Tavoni, M., 2017. The Shared Socioeconomic Pathways and their energy, land use, and greenhouse gas emissions implications: an overview. Global Environ. Change 42, 153–168.

Shindell, D., Kuylenstierna, J., Vignati, E., van Dingenen, R., Amann, M., Klimont, Z., Anenberg, S., Muller, N., Janssens-Maenhout, G., Raes, F., Schwartz, J., Faluvegi, G.,

Pozzoli, L., Kupiainen, K., Hoglund-Isaksson, L., Emberson, L., Streets, D., Ramanathan, V., Hicks, K., Oanh, N., Milly, G., Williams, M., Demkine, V., Fowler, D., 2012. Simultaneously mitigating near-term climate change and improving human health and Food security. Science 335 (6065), 183–189. https://doi.org/10.1126/science.1210026.

Stanaway, J.D., Afshin, A., Gakidou, E., Lim, S.S., Abate, D., Abate, K.H., et al., 2018. Global, regional, and national comparative risk assessment of 84 behavioural, environmental and occupational, and metabolic risks or clusters of risks for 195 countries and territories, 1990–2017: a systematic analysis for the Global Burden of Disease Study 2017. Lancet 392, 1923–1994. https://doi.org/10.1016/S0140-6736(18)32225-6.

Stevenson, D.S., Young, P.J., Naik, V., Lamarque, J.F., Shindell, D.T., Voulgarakis, A., Skeie, R.B., Dalsoren, S.B., Myhre, G., Berntsen, T.K., Folberth, G.A., Rumbold, S.T., Collins, W.J., MacKenzie, I.A., Doherty, R.M., Zeng, G., van Noije, T.P.C., Strunk, A., Bergmann, D., Cameron-Smith, P., Plummer, D.A., Strode, S.A., Horowitz, L., Lee, Y. H., Szopa, S., Sudo, K., Nagashima, T., Josse, B., Cionni, I., Righi, M., Eyring, V., Conley, A., Bowman, K.W., Wild, O., Archibald, A., 2013. Tropospheric ozone changes, radiative forcing and attribution to emissions in the atmospheric chemistry and climate model intercomparison project (ACCMIP). Atmos. Chem. Phys. 13, 3063–3085.

Turner, M.C., Jerrett, M., Pope, C.A., Krewski, D., Gapstur, S.M., Diver, W.R., Beckerman, B.S., Marshall, J.D., Su, J., Crouse, D.L., Burnett, R.T., 2016. Long-term ozone exposure and mortality in a large prospective StudyAm. J. Respir. Crit. Care Med. 193, 1134–1142. https://doi.org/10.1164/rccm.201508-1633OC.

United Nations Environment Programme (Unep), 2019. Air Pollution and Human Health: the Case of the Western Balkans. https://www.developmentaid.org/api/frontend/cms/uploadedImages/2019/06/Air-Quality-and-Human-Health-Report_Case-of-Western-Balkans_preliminary_results.pdf.

Van Dingenen, R., Dentener, F.J., Raes, F., Krol, M.C., Emberson, L., Cofala, J., 2009. The global impact of ozone on agricultural crop yields under current and future air quality legislation. Atmos. Environ. 43, 604–618. https://doi.org/10.1016/j.atmosenv.2008.10.033.

Van Dingenen, R., Dentener, F., Crippa, M., Leitao, J., Marmer, E., Rao, S., Solazzo, E., Valentini, L., 2018. TM5-FASST: a global atmospheric source–receptor model for rapid impact analysis of emission changes on air quality and short-lived climate pollutants. Atmos. Chem. Phys. 18, 16173–16211.

van Marle, M.J.E., Kloster, S., Magi, B.I., Marlon, J.R., Daniau, A.L., Field, R.D., Arneth, A., Forrest, M., Hantson, S., Kehrwald, N.M., Knorr, W., Lasslop, G., Li, F., Mangeon, S., Yue, C., Kaiser, J.W., van der Werf, G.R., 2017. Historic global biomass burning emissions for CMIP6 (BB4CMIP) based on merging satellite observations with proxies and fire models (1750–2015), Geosci. Model Dev 10, 3329–3357. https://doi.org/10.5194/gmd-10-3329-2017.

Wang, X., Mauzerall, D.L., 2004. Characterizing distributions of surface ozone and its impact on grain production in China, Japan and South Korea: 1990 and 2020. Atmos. Environ. 38 (26), 4383–4402. https://doi.org/10.1016/j.atmosenv.2004.03.067.

World Bank, 2021. World development indicators database. http://data.worldbank.org/data-catalog/world-development-indicators.

World Health Organisation (Who), 2020. AirQ+: Software Tool for Health Risk Assessment of Air Pollution. https://www.euro.who.int/en/health-topics/environment-and-health/air-quality/activities/airq-software-tool-for-health-risk-assessment-of-air-pollution. (Accessed 9 February 2021). latest access.